Future heat vulnerability in California, Part I: projecting future weather types and heat events

Scott C. Sheridan, Cameron C. Lee, Michael J. Allen & Laurence S. Kalkstein

Climatic Change
An Interdisciplinary, International Journal Devoted to the Description, Causes and Implications of Climatic Change

ISSN 0165-0009
Volume 115
Number 2

Climatic Change (2012) 115:291-309
DOI 10.1007/s10584-012-0436-2

Springer

Climatic Change (2012) 115:291–309
DOI 10.1007/s10584-012-0436-2

Future heat vulnerability in California, Part I: projecting future weather types and heat events

Scott C. Sheridan · Cameron C. Lee · Michael J. Allen · Laurence S. Kalkstein

Received: 13 June 2011 / Accepted: 29 February 2012 / Published online: 21 March 2012

Abstract Excessive heat significantly impacts the health of Californians during irregular but intense heat events. Through the 21st century, a significant increase in impact is likely, as the state experiences a changing climate as well as an aging population. To assess this impact, future heat-related mortality estimates were derived for nine metropolitan areas in the state for the remainder of the century. Here in Part I, changes in oppressive weather days and consecutive-day events are projected for future years by a synoptic climatological method. First, historical surface weather types are related to circulation patterns at 500mb and 700mb, and temperature patterns at 850mb. GCM output is then utilized to classify future circulation patterns via discriminant function analysis, and multinomial logistic regression is used to derive future surface weather type at each of six stations in California. Five different climate model-scenarios are examined. Results show a significant increase in heat events over the 21st century, with oppressive weather types potentially more than doubling in frequency, and with heat events of 2 weeks or longer becoming up to ten times more common at coastal locations.

1 Introduction

Much of the state of California (USA) currently experiences a number of hot days each year, as well as significant excessive heat episodes, most recently in 2006 (Gershunov et al. 2009). These events are correlated with reduced air quality, prolonged and extreme heat, and elevated rates of human mortality and morbidity. Over the coming century, climate change is likely to alter the frequency and intensity of these events, and demographic change is expected to increase markedly the number of people vulnerable to these events. These changes are expected to significantly affect public health across the state.

S. C. Sheridan (✉) · C. C. Lee · M. J. Allen
Department of Geography, Kent State University, Kent, OH, USA
e-mail: ssherid1@kent.edu

L. S. Kalkstein
Department of Geography and Regional Studies, University of Miami, Coral Gables, FL, USA

The IPCC (Meehl et al. 2007) projects that globally, temperatures by the end of the 21st century when compared with the end of the 20th century are expected to be from 1.1 °C to 2.9 °C higher using a relatively environmentally friendly scenario (B2), and from 2.4 °C to 6.4 °C higher using a higher-emissions scenario (A1FI). These increases contain a sizable spatial variability, and are generally larger over land, as well as over more poleward latitudes. Research has also suggested changes in atmospheric circulation, with future climate change projecting onto the dominant modes of atmospheric variability such as the Arctic and North Atlantic Oscillations that already affect climate over North America (Stone et al. 2001; Gillett et al. 2003), as well as El Niño/Southern Oscillation-like patterns (Boer et al. 2004).

Specific modeling of excessive heat events in the future has been less studied; aside from global changes in the radiative balance and circulation changes, other regional considerations such as soil moisture may play a role (Clark et al. 2006). A key question is the role of climate variability, and the relative roles of changes in the mean and variance of future temperature patterns. Schär et al. (2004) address this directly, in their analysis of the 2003 European heat event in the context of future climate scenarios, showing a nearly 100 % increase in climate variability in future GCM scenarios relative to control runs, and a spatial pattern of temperature variability change that is entirely different from that of the mean temperature increase. Ballester et al. (2010) reach a different conclusion, suggesting future heat events will increase in proportion with the mean temperature increase. Gosling et al. (2011), using a perturbed-physics ensemble simulation, suggest that in projecting impacts of future heat waves, model physics uncertainty leads to greater discrepancies than emissions scenario uncertainty. Nevertheless, several studies (Stott et al. 2004; Beniston 2004; Beniston 2007; Kyselý 2009; Barriopedro et al. 2011) suggest that with circulation changes associated with climate change, heat waves similar to the 2003 event may be relatively commonplace by the end of the 21st century. Beyond temperature changes, Willett and Sherwood (2011) show that in estimating future heat vulnerability, the frequency of threshold exceedances depend strongly on relative humidity values as well.

Several studies have also examined future changes in heat events over North America. As part of a global analysis of weather extremes, Tebaldi et al. (2006) and Meehl and Tebaldi (2004) show a significant increase in the frequency and intensity of heat events in the future, with three-day events more than 3 °C warmer than present across interior California. Clark et al. (2006) show a large amount of variability in predicted heat events, with the largest increases across the northern US, but with increases over California between 2 °C and 8 °C. In a precursor to the present study (Hayhoe et al. 2004), heat extremes for five cities in California were analyzed. By the 2090s, average inland heat-wave intensity increases at nearly double the rate of coastal cities under both the B1 and A1FI scenarios. As the total number of heat-wave days is approximately equal across all locations, this indicates much hotter heat waves for inland cities, and a disproportionate increase in long-duration heat waves by the 2090s.

In this research, we develop estimates of projected changes in heat events and in heat-related mortality over the next century for nine major urban regions in California, based on historical observed relationships between large-scale weather patterns and region-specific mortality rates. Here in Part I, we describe the future changes to heat event frequency; in Part II, we develop heat-related mortality estimates from these changes.

Our framework for analyzing hot weather and heat events in this research is rooted in synoptic climatology, in particular, the Spatial Synoptic Classification (SSC; Sheridan 2002), a weather-type classification scheme that categorizes surface weather conditions at a given location into one of several weather types. The SSC is presently utilized in more than

four dozen Heat Watch-Warning Systems (HWWS; Sheridan and Kalkstein 2004) and has already been employed and validated (Ebi et al. 2004; Hajat et al. 2010) in understanding heat events, and estimating heat-related mortality for purposes of calling heat advisories and warnings when human health is negatively impacted.

Rather than basing our analyses on surface predictions generated from downscaled atmosphere–ocean global climate model (GCM) output, we have associated GCM projections of synoptic scale, mid-tropospheric patterns with their likelihood of manifesting oppressive SSC weather types at the surface, a procedure new to future heat-health projections. As GCMs are better able to project general atmospheric patterns than localized weather variables (e.g., Wetterhall et al. 2009; Sheridan and Lee 2010), capitalizing on the relationships we derive enables us to more effectively and appropriately utilize model output in projecting future surface heat events and health impacts.

2 Materials and methods

2.1 Materials

2.1.1 Spatial Synoptic Classification

The Spatial Synoptic Classification (SSC) is a station-based weather-type classification scheme (Sheridan 2002), where each day is classified into one of six weather types: DM (Dry Moderate), DP (Dry Polar), DT (Dry Tropical), MM (Moist Moderate), MP (Moist Polar), or MT (Moist Tropical). These weather types are intended to represent a holistic categorical assessment of the weather conditions at a given location on a given day, and are based on surface observations of temperature, dew point, sea-level pressure, wind speed and direction, and cloud cover four times daily (0100, 0700, 1300, 1900 local standard time [LST]). The SSC is a hybrid classification scheme, with an initial manual specification of typical weather-type conditions leading to the identification of 'seed days' that typify each weather type during each season. An automated classification then ensues, whereby all days in a period of record are assigned to one of the weather types based on their similarity to the seed days. Complete details of the procedures that comprise weather-type classification with the SSC can be found in Sheridan (2002). Following classification into one of the weather types listed above, the SSC can then re-categorize those days with large pressure or dew point changes (usually representing the presence of a mid-latitude cyclone) as a transitional type (TR). Given the diversity of conditions on such days, and its lack of relevance to the focus of this study (heat events), only the six original SSC categories were used. As discussed further in Part II, the two tropical weather types—MT and DT—are associated with excess mortality and hence will be referred to as the 'oppressive' weather types.

Historical SSC "calendars" (where each day in a period of record is classified into one weather type) are available for over 400 first-order stations globally (http://sheridan.geog.kent.edu/ssc.html), including 18 in California. As the study area for this project includes nine urbanized regions in California (Fig. 1), extensive preliminary testing was done to evaluate the most appropriate SSC stations to use. The SSC surface weather type must be adequately predicted by upper-atmospheric circulation patterns in order for future projections to be appropriate, in particular the tropical weather types (DT and MT) that have most often been associated with increases in human mortality (Sheridan et al. 2009). Several large airport weather stations, such as Los Angeles (LAX), San Francisco (SFO), and San Diego (SAN),

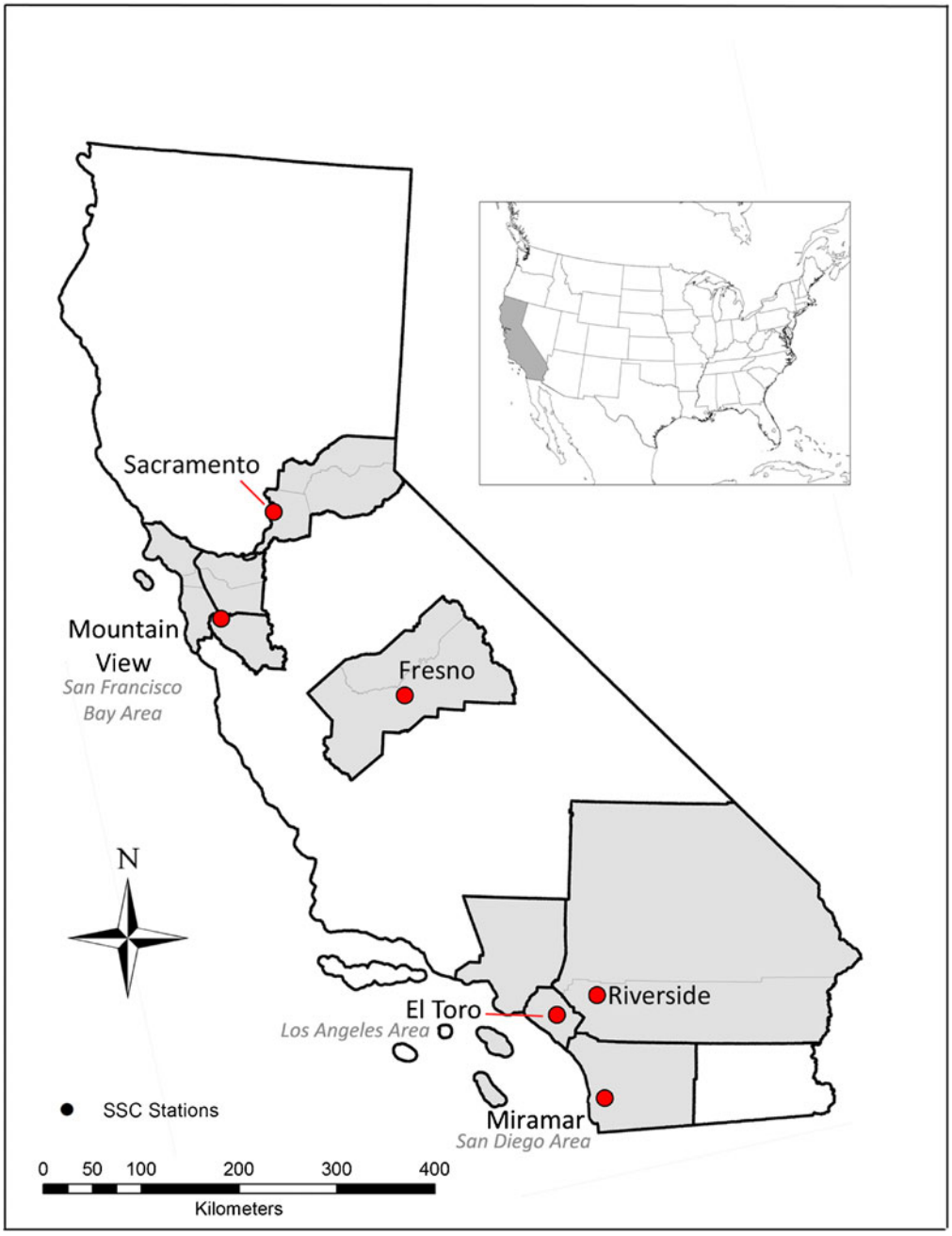

Fig. 1 The SSC stations used in this research. The population regions used in Part II are *shaded*

are located directly adjacent to the coastline, and surface weather type can be significantly affected by a sea breeze that is difficult to predict using larger-scale atmospheric circulation. The stations chosen instead for these coastal locations—somewhat inland from the aforementioned

stations—are more representative of the population centers. The six stations ultimately chosen are shown in Fig. 1; mean DT and MT conditions are depicted in Table 1. As shown in the results, weather types at all of these stations can successfully be estimated from larger-scale circulation patterns.

It should be noted here that our use of the term 'heat event' as a representation of all DT and MT days is by virtue of our framework. Since MT and DT weather types vary across space and time, no standard definition of a heat event in terms of temperature threshold can be provided.

2.1.2 Historical atmospheric circulation and temperature data

One of the most common historical weather data sets available is the NCEP/NCAR reanalysis (NNR) data set (Kalnay et al. 1996), which includes many variables for the global domain across many layers of the atmosphere. Though the data are derived from both actual observations as well as short-term model simulations, and have some inherent biases, the

Table 1 Mean (standard deviation) conditions for Dry Tropical ("DT") and Moist Tropical ("MT") weather types in April, June, and August, for the stations used in this study, for the 1960–1999 observed historical period. "1300" and "0100" values are the temperature (T, °C) and dew point (Td, °C), for those hours (LST) respectively, while "Freq" refers to the mean monthly frequency of occurrence, as a percentage of all days

Station		April			June			August		
		1300	0100	Freq	1300	0100	Freq	1300	0100	Freq
El Toro	DT T	29 (3)	15 (3)	10 %	34 (3)	20 (3)	4 %	35 (2)	22 (2)	5 %
	DT Td	5 (5)	3 (5)		11 (3)	10 (3)		14 (3)	13 (3)	
	MT T	23 (3)	15 (1)	17 %	27 (3)	18 (1)	6 %	30 (2)	20 (1)	20 %
	MT Td	12 (2)	11 (2)		17 (2)	16 (1)		19 (2)	17 (1)	
Fresno	DT T	28 (3)	14 (3)	19 %	35 (3)	22 (3)	41 %	36 (2)	24 (2)	42 %
	DT Td	5 (4)	6 (4)		10 (4)	10 (4)		12 (3)	13 (3)	
	MT T	21 (2)	15 (2)	1 %	30 (3)	23 (3)	1 %	30 (2)	25 (2)	1 %
	MT Td	10 (3)	11 (3)		14 (4)	14 (3)		16 (3)	14 (2)	
Miramar	DT T	28 (3)	14 (3)	7 %	33 (3)	19 (2)	3 %	33 (2)	21 (2)	2 %
	DT Td	4 (4)	3 (4)		9 (4)	10 (5)		13 (3)	14 (3)	
	MT T	23 (3)	14 (2)	20 %	27 (2)	17 (1)	9 %	29 (2)	20 (1)	23 %
	MT Td	13 (2)	11 (2)		16 (2)	15 (1)		18 (1)	18 (1)	
Mountain View	DT T	25 (3)	14 (2)	14 %	31 (3)	18 (3)	8 %	32 (2)	20 (2)	2 %
	DT Td	5 (5)	5 (3)		10 (4)	10 (3)		10 (4)	12 (2)	
	MT T	21 (2)	14 (2)	14 %	26 (2)	18 (2)	6 %	28 (3)	21 (2)	1 %
	MT Td	11 (3)	10 (2)		14 (2)	13 (2)		17 (2)	16 (1)	
Riverside	DT T	29 (3)	12 (3)	20 %	35 (3)	17 (3)	25 %	36 (2)	20 (3)	39 %
	DT Td	0 (4)	3 (5)		7 (4)	9 (3)		10 (4)	11 (3)	
	MT T	23 (4)	14 (1)	7 %	32 (3)	18 (2)	9 %	34 (2)	21 (2)	17 %
	MT Td	11 (2)	10 (2)		15 (2)	14 (2)		16 (3)	15 (2)	
Sacramento	DT T	25 (3)	12 (3)	12 %	35 (3)	19 (3)	23 %	35 (2)	19 (2)	24 %
	DT Td	4 (5)	4 (5)		10 (4)	10 (3)		12 (3)	11 (2)	
	MT T	25 (3)	15 (1)	2 %	33 (3)	22 (2)	<1 %	30 (2)	24 (1)	<1 %
	MT Td	13 (3)	12 (2)		16 (2)	13 (2)		13 (4)	12 (3)	

data set is generally considered to be an appropriate representation of 'observed' historical conditions, particularly in terms of the atmospheric modes of variability that are assessed in this research, although systematic differences are still observed (e.g., Schoof and Pryor 2003). In this research, data from the NNR data set were obtained at a once-daily resolution (1200 UTC; 0400 LST) from 1 September 1957 to 31 August 2002, for the 500mb and 700mb geopotential height fields (500z and 700z respectively) and the 850mb temperature field (850t). These variables are commonly used in synoptic classifications (Sheridan and Lee 2010; Vrac et al. 2007) and are considered among the more reliable variables in the NNR data set (Kalnay et al. 1996). These fields are also considered appropriate for the evaluation of surface heat events. The geopotential height field at the 500mb level is useful for examining the overall trough and ridge pattern over the study area, indicative of larger-scale advection and subsidence in the atmosphere; the 700mb geopotential height values are strongly correlated with surface temperatures (Knapp 1992); and the 850mb temperatures are a good approximation of surface temperature as well. Due to the unique approach used in this research, there was no *a priori* assumption as to which of the levels would most accurately correspond to surface weather types better than others, and thus all three fields were considered in the analysis.

Data were interpolated to a 5° by 5° resolution from 46°N to 26°N latitude and from 108°W to 128°W longitude, which includes all of California. Due to the large amount of spatial autocorrelation of geopotential height and temperature data, the coarser grid is not likely to affect the results of a synoptic scale classification of circulation patterns. Additionally, previous synoptic research has shown better results with a coarser resolution (Demuzere et al. 2009; Saunders and Byrne 1999). Several other research studies have evaluated the impacts of different domain sizes and found that the choice of domain affects how patterns in the region of interest are identified (Demuzere et al. 2009; Hope et al. 2006). Several different domains were tested, and the domain chosen most adequately represented the array of upper-level circulation patterns across California; larger domains included the Rocky Mountains which contain noise irrelevant to California climate conditions, and smaller domains could not adequately resolve larger-scale circulation patterns.

2.1.3 Future atmospheric circulation and temperature data

Future atmospheric circulation and temperature data have been acquired from two GCMs: the Community Climate System Model 3 (CCSM3; Collins et al. 2006), and the Coupled Global Climate Model, or the CGCM3 (Environment Canada 2009a, b) run by the Canadian Centre for Climate Modeling and Analysis. We utilized three of the six IPCC (2007) scenarios (from the Special Reports on Emissions Scenarios; SRES) in this research: A1FI ("higher emissions"), A2 ("mid-high emissions"), and B1 ("lower emissions"). For CCSM3, all three scenarios were used, while for CGCM3, only A2 and B1 were used. Thus, five total model-scenarios were analyzed. Projections were acquired through 2099 in all scenarios with CCSM3, and in two windows from 2045–2064 to 2081–2100 for CGCM3. Historical model runs, produced to verify the ability of GCMs to simulate present-day climate and climate variability, were also acquired. The 20th Century run of the CCSM3 GCM was taken from the same 1957–2002 time period as the NNR data, while the CGCM3 GCM historical time period spanned only from 1961 to 2000. GCM data were interpolated to the same resolution (5° by 5°) over the same domain (46°N to 26°N latitude and from 108°W to 128°W), and for the same variables at the three pressure height levels (500z, 700z, 850t).

2.2 Methods

2.2.1 Circulation type determination

The first stage in this research involved the categorization of upper-level patterns into clusters. The patterns were classified using a six-part process described fully in Lee and Sheridan (2011). In short, for each of the three levels of the atmosphere used in this research, principal components analysis and two-step cluster analysis were performed in SPSS to categorize historical weather conditions on each day in the NNR data set into one of several clusters. An example of clusters derived from the 700z dataset is in Fig. 2. Discriminant function analysis (DFA) was then utilized to categorize both historical and future GCM data for both the NNR and GCMs into the same clusters. The process is performed individually for each of the 15 combined (the 5 model-scenarios × the 3 levels of atmosphere) data sets. Cluster numbers, as well as leading principal-component scores, are both utilized later.

Better correlations between the patterns created with the NNR dataset and those created with a GCM's historical 20th Century (hereafter referred to as GCM20c) dataset were ultimately found only after 'debiasing' the GCM data; that is, removing the mean model bias at each grid point. This method has been successfully used in other literature (e.g., Hope 2006; Lee and Sheridan 2011; Lee 2011). For each grid point for both GCMs, the mean monthly difference between the GCM20c and the NNR data set in the historical period was removed from the GCM historical dataset. The same difference was then subtracted from the relevant future scenarios. The debiasing of the dataset resulted in statistically similar frequencies of weather types (shown below) and suggests that the debiased GCM data adequately represent climate variability as well as mean conditions.

In this research, a 9-month warm season (March to November) was delineated, and classification was performed only on these months. Several factors contribute to this decision. As synoptic variability is greatest during the cold season (Barnston and Livezey 1987), year-round classifications tend to create more winter patterns at the expense of summer patterns. As this research aims to identify heat events, this additional discrimination is not desired. Moreover, our previous research (e.g., Sheridan and Kalkstein 2010) suggests

Fig. 2 Mean geopotential height values (m) at 700mb for 700z clusters created in CCSM3

a relatively broad season during which heat-related mortality can occur, given California's unique climate. Further, as significant heat events in California can occur outside of the meteorological summer, and the seasonality of synoptic patterns may shift in the future (e.g., Lee 2011), this broad definition of warm season is necessary.

2.2.2 Using multinomial logistic regression to predict SSC weather-type

After the atmospheric circulation patterns were classified for each of the five model scenarios, the next step was to predict the daily SSC type for the GCM-Future data based upon the relationship of the atmospheric circulation patterns to SSC type in the historical NNR dataset. A dataset that includes historical weather-type data for each of the 6 SSC stations was then created for each of the 5 model-scenarios, creating a total of 30 datasets. We then tested multiple combinations of variables (Table 2): the cluster numbers for each of the three levels (500z, 700z, and 850t), including one-day lag and one-day lead; the three PC values for each level, along with one-day lags, and the actual 850-mb temperature values at two grid cells (36°N, 123°W; 36°N, 118°W). Finally, as meteorological conditions within each weather type vary over the course of the year, a seasonally oscillating variable was created that was defined as the sine of the seasonal cycle as reflected in the SSC—a value of 1 (−1) for the warmest (coldest) weather-type day of the year at a given station.

A custom multinomial logistic regression (MLR) was then used to project the SSC type for both the GCM20c portion of the data and the GCM Future portion of the data. MLR can use both continuous and categorical independent variables in order to predict the occurrence of a categorical dependant variable. The combination of variables that best reproduced historical weather-type frequencies at each station (minimizing the mean frequency differential for each weather type) was selected (marked by 'X' in Table 2). For the two Central Valley SSC stations, Sacramento and Fresno, the 850t level proved to be the only level important in predicting surface SSC type, and so information from the 500-mb and 700-mb levels was not included. For these two stations, five interaction terms were also added to the regression equation in order to characterize the combined effects of the daily DFA pattern with a number of different variables in determining surface weather type: 1) the 850t DFA number and the one-day lag of the 850t DFA number; 2) the 850t DFA number and the one-day lead of the 850t DFA number; 3) the 850t DFA number and the season-cycle curve; 4) the 850t DFA number and the 850t value at 36°N, 123°W; and 5) the 850t DFA number and the 850t value at 36°N, 118°W.

For the other four stations, the SSC type for these stations was as dependent on the 500-mb and 700-mb geopotential height patterns as the 850-mb temperature pattern, and thus the set of predictive variables was different (Table 2). Different interaction terms were also used: 1) the 700z DFA number with the 700z DFA one-day lag; 2) the 700z DFA number with the 700z DFA one-day lead; 3) the 700z DFA number with the month; 4) the 700z DFA number with the 850t at 36°N, 123°W; and 5) the 700z DFA number with the 850t at 36°N, 118°W.

3 Results

Given California's broad range of climates, weather-type frequencies vary considerably among the stations evaluated in this study (Table 1). Dry Tropical (DT) air dominates the summer in Fresno, Riverside, and Sacramento, while Moist Tropical (MT) air is more common at Miramar, Mountain View, and El Toro. In northern California, MT air has a spring peak, especially at Mountain View. However, in southern California, which is influenced somewhat by the late-

Table 2 Predictive variables included in the multinomial logistic regression (MLR) analysis for SSC type (dependent variable) for each station

Variable	Fresno, Sacramento	Riverside, Los Angeles, El Toro, Miramar
Categorical variables		
The DFA cluster number for 700z		X
The DFA cluster number for 850t	X	X
The 1 day lag of the DFA cluster number for 700z		X
The 1 day lag of the DFA cluster number for 850t	X	X
The 1 day lead of the DFA cluster number for 700z		X
The 1 day lead of the DFA cluster number for 850t	X	X
Month		X
Continuous variables		
PC 1 value for 500z		X
PC 2 value for 500z		X
PC 3 value for 500z		X
PC 1 value for 700z		X
PC 2 value for 700z		X
PC 3 value for 700z		X
PC 1 value for 850t	X	X
PC 2 value for 850t	X	X
PC 3 value for 850t	X	X
One-day lag of PC 1 value for 500z		X
One-day lag of PC 2 value for 500z		X
One-day lag of PC 3 value for 500z		X
One-day lag of PC 1 value for 700z		X
One-day lag of PC 2 value for 700z		X
One-day lag of PC 3 value for 700z		X
One-day lag of PC 1 value for 850t	X	X
One-day lag of PC 2 value for 850t	X	X
One-day lag of PC 3 value for 850t	X	X
The 850t value at 36°N, 123°W	X	X
The 850t value at 36°N, 118°W	X	X
The sinusoidal curve of seasonality of SSC stations	X	X

summer Southwest Monsoon (Sheppard et al. 2002), MT frequencies are greater in the fall, particularly at Miramar, the southernmost SSC station used in this research.

3.1 Historical results

An evaluation of seasonal frequencies and biases (for the entire March through November period) shows that both the CCSM3 and CGCM3 models adequately duplicate the historical pattern frequencies of the NNR, which helps validate the future weather-type frequency estimates (Table 3). Comparing the actual average seasonal frequencies with the NNR and GCM20c models shows that rarely are the frequencies more than 5 % apart. Chi-square tests on the annual mean frequency of SSC types show no statistically significant differences

Table 3 Weather type frequency in percent (March-November) for each SSC station for the observed period ("Actual"), NNR reanalysis ("NNR") and the GCM historical and 2090–99 portion of future scenarios. Bold, italic values represent statistically significant differences ($p<.05$). In the NNR or GCM 20th century columns, differences are assessed between modeled SSC type frequency and observed weather type frequency. In the GCM Future columns, differences are assessed between GCM historical SSC frequency and future SSC frequency

	Obs. 1960–1999	NNR 1960–1999	CCSM3				Obs. 1970–1999	NNR 1970–1999	CGCM3		
			1960–1999	A1FI 2090–99	A2 2090–99	B1 2090–99			1970–1999	A2 2090–99	B1 2090–99
	Sacramento										
DM	58.2	53.1	54.8	***21.1***	***26.8***	***45.5***	58.4	59.5	61.9	***41.2***	***52.1***
DP	6.8	8.7	8.9	***1.0***	***1.5***	***4.0***	6.5	7.6	6.9	***0.4***	***2.2***
DT	20.9	19.9	18.3	***42.8***	***42.7***	***30.1***	21.0	18.9	18.0	***37.4***	***27.8***
MM	7.1	8.0	9.1	***12.1***	9.0	9.6	6.9	7.0	7.0	6.6	8.5
MP	5.3	5.8	4.4	***0.6***	***0.4***	***2.3***	5.0	4.2	3.3	***1.0***	2.0
MT	1.8	4.5	4.4	***22.4***	***19.5***	***8.5***	2.0	2.9	2.9	***13.4***	***7.4***
	Fresno										
DM	50.8	46.5	46.8	***27.0***	***32.2***	***43.1***	50.8	46.3	47.1	***31.9***	***39.5***
DP	9.0	11.3	11.7	***1.7***	***2.1***	***5.9***	8.0	10.2	11.0	***2.2***	***4.2***
DT	30.5	28.7	27.6	***54.6***	***54.5***	***39.9***	31.2	29.1	28.3	***52.6***	***41.6***
MM	5.2	5.1	6.0	*3.5*	*3.2*	*4.9*	5.3	5.2	6.0	3.3	6.5
MP	2.5	***6.0***	4.9	***0.3***	***0.2***	***2.0***	2.4	***5.8***	4.6	***1.2***	***1.7***
MT	2.0	2.4	2.9	***12.9***	***7.8***	4.2	2.2	3.4	2.9	***8.8***	***6.5***
	Riverside										
DM	36.5	34.6	33.7	***17.7***	***19.2***	27.8	36.7	32.6	32.3	***20.3***	***25.2***
DP	10.7	12.0	11.7	***1.6***	***1.8***	***5.6***	9.4	12.2	11.5	***2.1***	***4.9***
DT	29.7	33.1	33.0	***62.3***	***63.4***	***47.7***	29.5	32.8	33.5	***63.2***	***51.6***
MM	9.9	7.9	9.8	***4.7***	***4.1***	8.8	10.2	9.5	10.8	***5.1***	9.1
MP	3.6	6.4	7.0	***0.3***	***0.4***	***2.9***	3.5	5.9	6.4	***0.7***	***2.5***
MT	9.5	5.9	***4.8***	***13.4***	***10.9***	7.1	10.8	6.9	5.5	8.7	6.7

Table 3 (continued)

	Obs. 1960–1999	NNR 1960–1999	CCSM3				Obs. 1970–1999	NNR 1970–1999	CGCM3		
			1960-1999	A1FI 2090–99	A2 2090–99	B1 2090–99			1970–1999	A2 2090–99	B1 2090–99
	Mountain View										
DM	55.1	59.1	54.4	***28.3***	***33.3***	47.4	58.1	64.0	59.3	***51.2***	54.6
DP	1.6	***5.2***	***5.0***	***0.2***	***0.3***	***2.2***	1.2	3.7	3.3	***0.1***	0.7
DT	7.6	10.5	11.1	***18.8***	***20.8***	14.4	8.5	9.8	11.6	***15.6***	13.3
MM	16.8	12.0	14.2	19.2	18.5	***19.5***	15.4	***10.6***	13.4	11.9	14.7
MP	10.9	***4.5***	***6.1***	***0.3***	***0.2***	***1.8***	7.9	***3.3***	***4.3***	***0.1***	***0.5***
MT	8.0	8.8	9.1	***33.3***	***27.0***	***14.6***	9.0	8.6	8.1	***21.1***	16.2
	El Toro										
DM	50.4	***67.7***	***66.1***	***41.5***	***42.1***	59.9	48.8	***60.8***	***59.5***	***41.5***	54.6
DP	2.4	1.1	1.3	0.2	***0.0***	0.4	2.1	3.8	3.8	***0.6***	***1.0***
DT	10.8	7.2	7.7	***15.1***	***16.6***	10.3	11.2	8.4	8.8	***18.7***	***14.1***
MM	15.7	11.9	13.6	***5.5***	***4.6***	9.7	16.3	12.3	13.6	***3.8***	***8.9***
MP	6.8	***3.1***	***3.4***	***0.3***	***0.2***	***1.1***	5.7	5.0	4.9	***0.3***	***1.8***
MT	13.9	9.1	***7.8***	***37.4***	***36.5***	***18.5***	16.0	9.7	9.4	***35.2***	***19.5***
	Miramar										
DM	54.3	53.7	53.7	***24.8***	***28.2***	44.7	55.2	55.3	54.9	***31.5***	45.5
DP	2.2	***7.2***	***7.2***	***0.5***	***0.4***	***2.7***	2.5	***6.2***	***5.3***	***0.5***	***2.1***
DT	6.5	9.3	10.0	***21.3***	***23.7***	13.6	6.5	10.1	***10.8***	***21.4***	***16.7***
MM	14.5	12.2	12.8	***8.7***	***7.3***	11.1	12.9	11.9	11.5	***4.9***	8.1
MP	6.6	7.1	6.6	***0.4***	***0.3***	***3.4***	6.2	6.7	7.3	***1.0***	***3.4***
MT	15.9	***10.6***	***9.7***	***44.3***	***40.0***	***24.5***	16.8	***9.8***	***10.2***	***40.6***	***24.2***

between the NNR and GCM20c frequencies, for either CGCM3 or CCSM3. Statistically significant differences occur between the *observed* SSC frequencies and both models' GCM20c output at the three coastal locations; differences are also observed between the GCM20c output and observed frequencies for Riverside for the CCSM3 only. When examining the statistical differences by SSC type, the majority of the cases in which differences are observed are the polar weather types, especially MP. Since this research is primarily interested in the frequency of tropical weather types, differences in polar frequencies are less critical. Only a few differences in tropical weather types emerge: at Miramar, the NNR and both GCMs systematically underrepresent MT (p=.02 to p=.05); the CGCM3 overrepresents DT at Miramar (p=.048), and the CCSM3 underrepresents MT at both Riverside (p=.022) and El Toro (p=.014).

3.2 Future results

3.2.1 Weather type frequencies

By the 2090s, all the model-scenarios suggest that polar weather types (DP, MP) largely disappear and the moderate weather types (DM, MM) decrease, while the overall frequency of the two tropical weather types is projected to increase substantially (Table 3), though with large differences across the model-scenarios. For the A1FI and A2 scenarios, DT roughly doubles in frequency across all stations except Mountain View, with the largest absolute increase observed at Riverside with CCSM A2, where it is projected to occur on 63.4 % of all days, compared with 33.0 % in the GCM historical period. MT increases under A1FI and A2 are more substantial in percentage terms than the DT increases, with MT generally doubling at Riverside and becoming five times as common at Sacramento. The B1 scenario is associated with a far more muted response overall, yet tropical types are still projected to increase, with MT doubling in frequency relative to the GCM historical period in several cases.

In holding the scenario constant, the two GCMs show broadly similar rates of increase. Both models show the greatest increases at Sacramento, El Toro, and Miramar. The CCSM3 is associated with greater DT increases under the A2 scenario than the CGCM3; conversely, for MT under B1, the CGCM3 shows much greater percentage increases than the CCSM3 across the three northernmost stations in Sacramento, Fresno, and Mountain View.

On a seasonal level, the oppressive weather types are projected to become more frequent during the seasons in which they normally occur, and broaden the range of the season in which they appear (Fig. 3). In the more inland locations of Fresno, Riverside, and Sacramento, there is projected to be a marked increase in summertime DT frequency beyond the already high levels. In Fresno, DT is projected to become almost totally predominant, reaching frequencies of over 80 % during the 2090s under all scenarios in both models, and approaching 100 % of all days in the CCSM3 A1FI scenario. Sacramento and Riverside show large increases as well, with most scenarios showing midsummer DT frequency above 80 %; in the case of Sacramento, the peak DT frequency is projected to expand its seasonality to even earlier in the summer, into July and August. While the most substantial increases in DT frequency in Fresno and Sacramento are found in midsummer, in Riverside, increases are of similar magnitude throughout the entire 9-month period.

In these inland cities, MT is much less common historically, and is projected to remain relatively uncommon—with two noted exceptions. At Sacramento and Fresno, where MT is

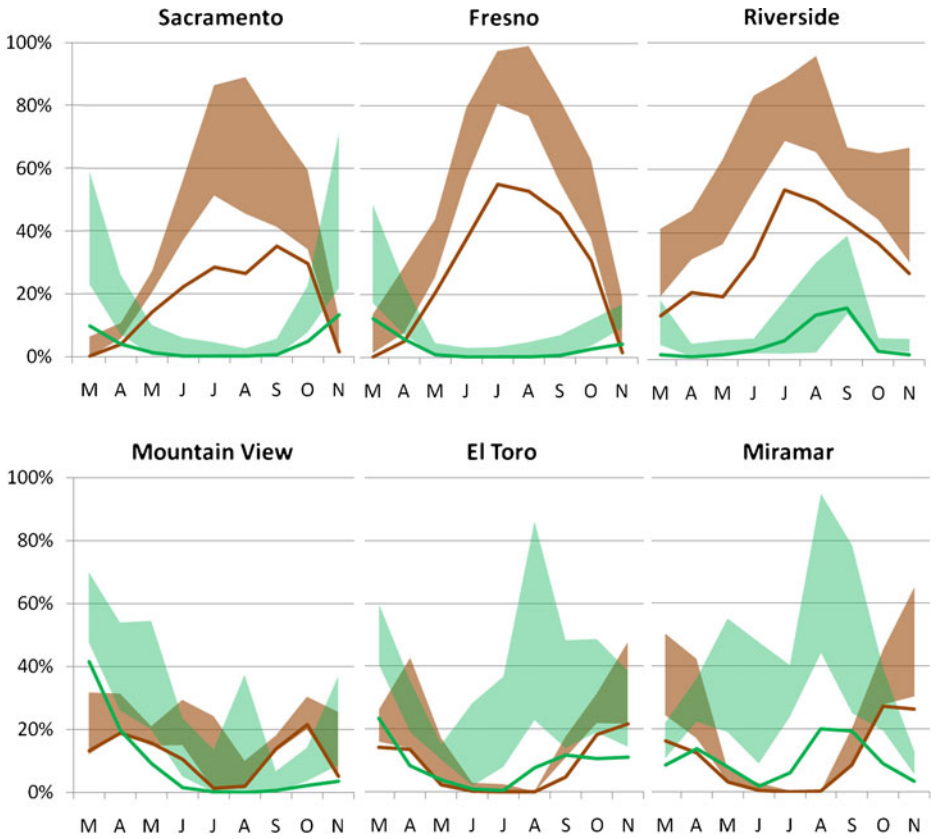

Fig. 3 Monthly frequency of the GCM-modeled DT (*brown*) and MT (*green*) weather types at each station for the historical period (*solid line*) and the 2090s range across all 5 GCM scenarios utilized in this research (*shaded area*)

most common in the transitional seasons, there are indications that MT frequency will increase rather sharply during early spring, with projected frequency at Fresno and Sacramento as high as 45 and 60 % of March days, respectively, in the 2090s in the CCSM3 A1FI scenario. At Riverside, presently marginally affected by the Southwest Monsoon in late summer, MT frequency doubles in August and September in the more aggressive A1FI and A2 scenarios compared with the GCM historical period, while in the B1 scenario, almost no change in MT frequency is observed by the 2090s.

For the coastal cities, the pattern is generally inverted, with broader overall increases observed in MT rather than DT. Early and late season MT is projected to increase at all three stations, especially Mountain View and El Toro, with a relatively narrow range among model-scenarios. Frequencies in late-summer and early-autumn MT weather-type days vary considerably by model-scenario, with a substantially greater increase in the A1FI and A2 scenarios at El Toro and Miramar than in B1. At Mountain View, MT does not presently occur during this same time of year, though in the A1FI and A2 scenarios, it appears by the 2090s in August.

DT frequency at the coastal cities is projected to increase as well, although in the B1 scenario this increase is slight. A general increase is observed at Mountain View across all

months, while at Miramar and El Toro, DT increases are largely observed in the transitional seasons, when Santa Ana winds, adiabatically warmed air advected from the desert to the Pacific coast via an anticyclone over the Great Basin to the east (Raphael 2003), are most common. In these cases, model-scenario variability is substantial, with much greater increases in the A1FI and A2 scenarios, in which the frequency more than doubles.

In terms of trends through the 21st century, there is considerable variability among the scenarios (Fig. 4). Overall, through the 2040s, there is little divergence between the scenarios; linear increases are generally observed only in the DT weather type inland and the MT weather type at coastal stations. From the 2050s through the 2090s, under the A1FI and A2 scenarios, both weather types increase linearly with a greater slope than earlier in the century. With B1, however, there are no statistically significant increases in the number of DT or MT days from the 2040s to the 2090s at any of the stations. In comparing the two GCMs across similar scenarios, systematic differences are only observed at the two northernmost cities, Sacramento and Mountain View; in both of these cases, the CGCM3 A2 scenario projects significantly fewer DT and MT days in the 2090s.

3.2.2 Heat events

At present, the largest number of oppressive days occurs at the inland sites of Fresno, Riverside, and Sacramento, with Riverside clearly being the highest in all models

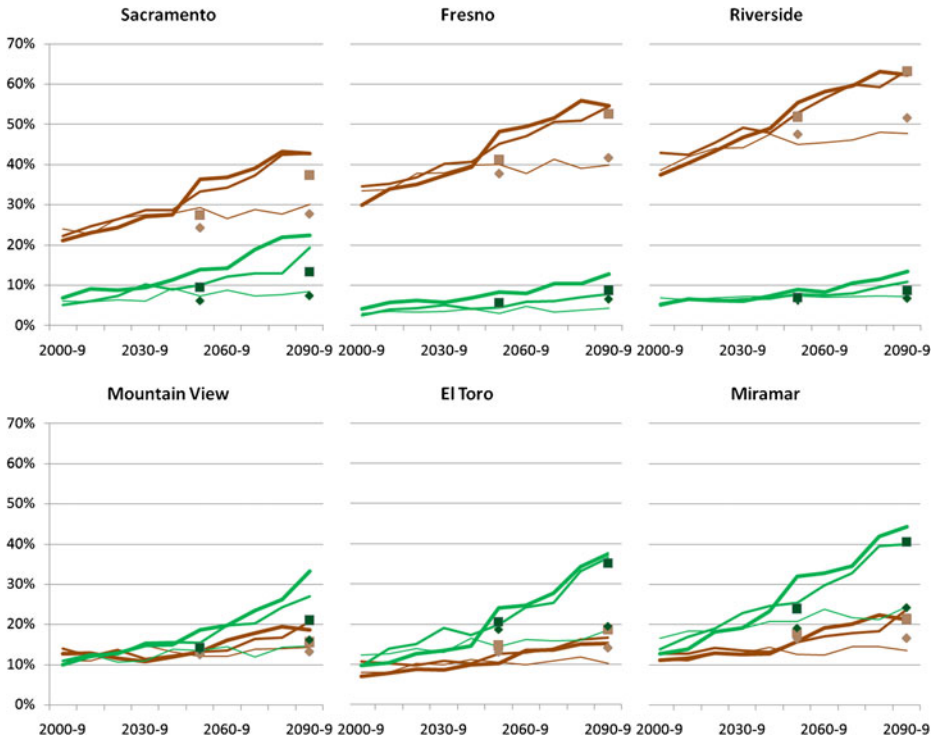

Fig. 4 Decadal frequency of the GCM-modeled DT (*brown*) and MT (*green*) weather types at each station for the 21st century across all 9 months used in analysis. *Thickest line* is CCSM A1FI scenario; *mid-weight line* is CCSM A2 scenario; *thin line* is CCSM B1 scenario. CGCM A2 scenario is shown with *filled box*; CGCM B1 scenario is shown with *filled diamond*

Table 4 Average annual total oppressive weather-type days (DT or MT; "Days"), annual occurrence of consecutive-day runs of at least 7 days ("7-day") and 14 days ("14-day") for each SSC station for the observed period ("Actual"), NNR reanalysis ("NNR") and the GCM historical and future runs

SSC	NNR 1960–1999	CCSM3							NNR 1970–1999	CGCM3				
		1960–1999	A1FI		A2		B1			1970–1999	A2		B1	
			2050s	2090s	2050s	2090s	2050s	2090s			2050s	2090s	2050s	2090s
El Toro														
Days	44.4	42.5	93.8	143.4	86.8	142.6	68.0	78.6	49.3	49.8	96.4	147.2	86.6	91.7
7-day	1.4	1.1	4.3	7.0	3.8	7.1	2.2	3.6	1.5	1.2	3.8	8.1	4.0	3.2
14-day	0.2	0.2	1.0	2.2	0.5	2.0	0.2	1.0	0.1	0.1	0.6	2.1	0.8	0.4
Fresno														
Days	84.9	83.5	154.2	184.2	135.1	170.1	117.6	120.5	88.7	85.3	128.1	167.7	117.2	131.5
7-day	3.7	3.6	5.4	5.8	5.4	5.4	5.3	4.7	3.9	3.4	6.0	7.3	5.0	5.2
14-day	1.0	0.7	2.6	2.9	2.2	2.2	2.2	1.6	1.1	0.8	1.8	3.2	1.6	1.8
Miramar														
Days	54.1	53.7	130.5	179.0	112.4	174.1	91.1	103.9	54.4	57.4	114.3	169.3	97.3	111.7
7-day	1.5	1.5	5.9	9.1	4.9	8.3	3.7	4.3	1.2	1.3	5.2	8.3	3.5	4.6
14-day	0.1	0.1	1.8	3.1	0.8	3.1	0.3	1.0	–	0.1	0.7	2.8	0.6	0.7
Mountain View														
Days	52.7	55.3	87.1	142.2	78.5	130.4	70.2	79.3	50.1	53.8	76.8	100.2	71.3	80.5
7-day	1.5	1.8	3.8	5.6	3.4	5.1	2.7	3.4	1.1	1.4	2.4	4.0	2.2	2.8
14-day	0.4	0.4	1.0	1.9	0.4	2.0	0.6	0.7	0.2	0.1	0.4	0.6	0.2	0.2
Riverside														
Days	106.6	103.2	175.4	206.7	165.6	203.0	142.9	149.7	108.5	106.5	160.6	196.3	146.8	159.2
7-day	4.7	4.3	6.4	6.7	7.5	7.8	6.5	6.4	4.9	4.4	7.5	7.6	7.5	7.6
14-day	1.2	1.1	3.3	2.8	3.1	2.9	2.5	2.3	1.2	1.3	2.5	2.9	2.2	2.9
Sacramento														
Days	66.7	62.0	137.6	177.9	118.5	169.8	100.0	105.5	59.4	57.1	100.8	138.7	83.2	96.1
7-day	2.0	1.7	6.4	7.8	5.2	7.3	4.7	4.3	2.1	1.6	3.8	7.1	3.9	3.0
14-day	0.2	0.2	1.9	3.3	1.2	2.8	0.8	1.2	0.1	0.2	0.5	1.8	0.3	0.5

(Table 4). The estimates of future oppressive weather-type days show increases across all cities in this analysis, but the percentage differential between the locales diminishes, particularly for the 2090s. For example, from 1960 to 2000 the number of oppressive days per year varies from 44 in El Toro to 107 at Riverside, well over double. By the 2090s, under A1FI, the number of oppressive days per year ranges from 142 at Mountain View to 207 at Riverside. Thus, all of California is projected to experience large numbers of offensive days under the worst case A1FI scenario, and even under the more conservative scenarios.

Commensurate with the increase in the number of oppressive days is a substantial increase in long consecutive-day events. Seven-day or longer events may more than double at the coastal sites in virtually all of the scenarios for the 2090s. At Miramar as an example, presently such events occur about 1.5 times during a typical nine-month season. This is projected to increase to 4.3 times for the most conservative B1 scenario by the 2090s. More substantial is the increase in frequency of events of at least 14 consecutive days, which are exceedingly rare now. Only at Riverside do such lengths of offensive days occur more than once a season at present. By the 2090s, these 14-day runs are projected to occur over once a year at virtually all the locales under almost all the model runs (with a few exceptions, generally for the B1 scenarios). The increase in frequency is estimated at tenfold or greater at some of the coastal locations.

4 Discussion

The methodology presented in this research involved a process whereby different historical upper-level circulation patterns were initially developed for each of the two GCMs, followed by a multinomial logistic regression to predict surface weather-type. That the results from the two GCMs are generally similar, despite the process being done independently for each GCM, suggests the methodology is robust.

Using the various GCM models and emissions scenarios, the results strongly suggest that the oppressive weather type days, DT and MT, are projected to occur even more frequently than they do today. Not surprisingly, the dry, generally clear, and hot DT weather type is projected to become much more frequent in Fresno, Riverside, and Sacramento—inland locales where atmospheric moisture is relatively low. The very warm and more humid MT weather type is projected to be more frequent in Miramar, Mountain View, and El Toro. Little difference is seen among model-scenarios through the 2040s, followed by a significant divergence. The A1FI scenario is associated with the largest increases, followed closely by A2; the B1 scenario has lesser increases, with almost no further increase after 2050. These results are broadly consistent with the only other known weather-type projections, using the SSC for Chicago (Hayhoe et al. 2010); the differences among SRES scenarios are similar to those of Hayhoe et al. (2004) for California using a temperature threshold; Tebaldi et al. (2006) show a similar divergence in scenarios, although in their research (which was aggregated globally), the divergence began 20 years earlier.

These results translate into a substantial rise in prolonged heat events. By the 2090s, 14- consecutive day runs of oppressive weather types are projected to occur about once a year at each station, while the frequency of 7-day heat events is projected to more than triple along coastal locations and increase more than 50 % inland under the higher emissions scenarios. While difficult to compare to previous research due to the different variables used, these results support research projecting more and longer-lasting heat events in the future (e.g., Meehl and Tebaldi 2004; Kyselý 2009; Barriopedro et al.

2011). One confounding factor, however, in estimating the number of consecutive-day heat events is that as heat events become more frequent, they are likely to begin merging. That is, while the total number of oppressive days is projected to increase, the number of 7-day or 14-day heat events might actually decrease as two or three separate events merge into one longer, single event.

In interpreting the results of the present study, we acknowledge the standard caveats about GCM ability to model future conditions and the scenarios representing plausible futures. Further, while there was broad agreement between the two GCMs used, there were certain areas of disagreement, such as with late summer MT frequency. More discrepancies may have been uncovered had additional GCMs been utilized. Other relevant work (Gosling et al. 2011) suggests that climate model physics represents a significant source of uncertainty as well, something not addressed in this work.

There are also some limitations that are specific to the research framework used here. We validated the methodology in terms of how well it was able to replicate historical observed weather type frequencies by using data from NNR or the historical portion of GCM runs. As discussed above, weather types were generally replicated well. There are some potential issues involving the historical period of record utilized. In comparing the weather types generated in the NNR portion of the classification (Table 2) for each of the two GCMs – run separately for somewhat different periods of record (1960–1999 vs. 1970–1999), different frequency biases (compared with the observed record) are noted, most notably at Sacramento and El Toro. When comparing the overlapping years in the two data sets, the only significant differences occur with the polar weather types. Since those types were not consequential in this research, we did not address this matter further; however, this discrepancy suggests that the selection of the historical period of record could impact classifications using this methodology.

Our results are based upon the assumption that the circulation-pattern—surface weather-type relationship remains the same in the future. Previous research has shown (Lee and Sheridan 2011) that the cluster means using the six-step method exhibit a slight drift into the future; that is, the shape of the patterns (such as those shown in Fig. 2) remains similar, but individual geopotential height/temperature values are all slightly higher. This would suggest the presented results may underestimate future heat events, although the inclusion of specific grid cell temperature values in the MLR equations may abate that somewhat.

One aim of future research along similar lines may be to enhance the spatial resolution and uniformity of the SSC. While the majority of the state's population does live near the six SSC stations selected for this project, a finer-scale gridded examination of weather types that extends beyond the urbanized areas analyzed herein could aid in the understanding of the small-scale impacts of climate change—and over a much wider spatial domain as well. Further, due to the widely varying topography of California and its correspondingly complex climate, a higher-resolution gridded weather-typing scheme could uncover more fine-scale nuances of the heat-health relationship.

To help assess the impacts of climate change on human health, the goal of this project has been to provide a range of 21st century heat-related mortality projections for nine major urban centers in the state of California. The implications that the results presented here may have for human mortality is shown in Part II.

Acknowledgments We would like to express our gratitude to the California Air Resources Board for their financial support of this research, especially Deborah Drechsler, our project manager. We also would like to acknowledge Katharine Hayhoe and Jeff Van Dorn for their provision of most of the raw NNR and GCM data. We thank the editors and three anonymous reviewers who helped make our manuscript stronger.

References

Ballester J, Rodo X, Giorgi F (2010) Future changes in Central Europe heat waves expected to mostly follow summer mean warming. Clim Dyn 98:277–284

Barnston AG, Livezey RE (1987) Classification, seasonality, and persistence of low-frequency atmospheric circulation patterns. Mon Weather Rev 115:1083–1126

Barriopedro D, Fisher E, Luterbacher J, Trigo RM, García-Herrera R (2011) The hot summer of 2010: redrawing the temperature record map of Europe. Science. doi:10.1126/science.1201224

Beniston M (2004) The 2003 heat wave in Europe: a shape of things to come?An analysis based on Swiss climatological data and model simulations. Geophys Res Lett 31. doi:10.1029/2003GL018857

Beniston M (2007) Entering into the "greenhouse century": recent record temperatures in Switzerland are comparable to the upper temperature quantiles in a greenhouse climate. Geophys Res Lett 34: L16710. doi:10.1029/2007GL030144

Boer GJ, Yu B, Kim SJ, Flato GM (2004) Is there observational support for an El Nino-like pattern of future global warming? Geophys Res Lett 31:art. no. L06201. doi:10.1029/2003GL018722

Clark R, Brown S, Murphy J (2006) Modeling northern hemisphere summer heat extreme changes and their uncertainties using a physics ensemble of climate sensitivity experiments. J Clim 19:4418–4435

Collins WD, Bitz CM, Blackmon ML, Bonan GB, Bretherton CS, Carton JA, Chang P, Doney SC, Hack JA, Henderson TB, Kiehl JT, Large WG, McKenna DS, Santer BD, Smith RD (2006) The Community Climate System Model: CCSM3. White paper, NCAR, Boulder, Colorado, USA

Demuzere M, Werner M, van Lipzig NPM, Roeckner E (2009) An analysis of present and future ECHAM5 pressure fields using a classification of circulation patterns. Int J Climatol 29:1796–1810

Ebi KL, Teisberg TH, Kalkstein LS, Robinson L, Weiher RF (2004) Heat watch/warning systems save lives: estimated costs and benefits for Philadelphia 1995–1998. Bull Am Meteorol Soc 85:1067–1073

Environment Canada (2009a) The Third Generation Coupled Global Climate Model (CGCM3), http://www.cccma.bc.ec.gc.ca/models/cgcm3.shtml. Accessed in January 2010

Environment Canada (2009b) The Third Generation Atmospheric General Circulation Model (AGCM3), http://www.cccma.bc.ec.gc.ca/models/gcm3.shtml. Accessed in January 2010

Gershunov A, Cayan DR, Iacobellis SF (2009) The great 2006 heat wave over California and Nevada: signal of an increasing trend. J Clim 22:6181–6203

Gillett NP, Allen MR, Williams KD (2003) Modeling the atmospheric response to doubled CO2 and depleted stratospheric ozone using a stratosphere-resolving coupled GCM. Q J R Meteorol Soc 129:947–966

Gosling SN, McGregor GR, Lowe JA (2011) The benefits of quantifying climate model uncertainty in climate change impacts assessment: an example with heat-related mortality change estimates. Clim Chang doi:10.1007/s10584-011-0211-9

Hajat S, Sheridan SC, Allen MJ, Pascal M, Laaidi K, Yagouti A, Bickis U, Tobias A, Bourque D, Armstrong BG, Kosatsky T (2010) Which days of hot weather are identified as dangerous by Heat-Health Warning Systems? A comparison of the predictive capacity of different approaches. Am J Publ Health 100:1137–1144

Hayhoe K, Cayan D, Field CB, Frumhoff PC, Maurer EP, Miller NL, Moser SC, Schneider SH, Cahill KN, Cleland EE, Dale L, Drapek R, Hanemann RM, Kalkstein LS, Lenihan J, Lunch CK, Neilson RP, Sheridan SC, Verville JH (2004) Emissions pathways, climate change, and impacts on California. Proc Natl Acad Sci 101:12422–12427

Hayhoe K, Sheridan SC, Kalkstein LS, Greene JS (2010) Climate change, heat waves, and mortality projections for Chicago. J Great Lakes Res 36:65–73

Hope PK (2006) Projected future changes in synoptic systems influencing southwest Western Australia. Clim Dyn 26:765–780

Hope PK, Drosdowsky W, Nicholls N (2006) Shifts in the synoptic systems influencing southwest Western Australia. Clim Dyn 26:751–764

Intergovernmental Panel on Climate Change (IPCC) (2007) Summary for policymakers. In: Parry ML, Canziani OF, Palutikof JP, van der Linden PJ, Hanson CE (eds) Climate change 2007: impacts, adaptation and vulnerability. Contribution of working group II to the fourth assessment report of the intergovernmental panel on climate change. Cambridge University Press, Cambridge, pp 7–22

Kalnay E, Kanamitsu M, Kistler R, Collins W, Deaven D, Gandin L, Iredell M, Saha S, White G, Woollen J, Zhu Y, Chelliah M, Ebisuzaki W, Higgins W, Janowiak J, Mo KC, Ropelewski C, Wang J, Leetmaa A, Reynolds R, Jenne R, Joseph D (1996) The NCEP/NCAR 40-Year reanalysis project. Bull Am Meteorol Soc 77:437–471

Knapp PA (1992) Correlation of 700mb height data with seasonal temperature trends in the Great Basin (western USA) 1947–1987. Clim Res 2:65–71

Kyselý J (2009) Recent severe heat waves in central Europe: how to view them in a long-term prospect? Int J Climatol 30:89–109

Lee CC (2011) Utilizing synoptic climatological methods to assess the impacts of climate change on future tornado-favorable environments. Nat Hazards in Press

Lee CC, Sheridan SC (2011) A six-step approach to developing future synoptic classifications based on GCM output. Int J Climatol in press. doi:10.1002/joc.2394

Meehl GA, Tebaldi C (2004) More intense, more frequent, and longer lasting heatwaves in the 21st century. Science 305:994–997

Meehl GA, Stocker TF, Collins WD, Friedlingstein P, Gaye AT, Gregory JM, Kitoh A, Knutti R, Murphy JM, Noda A, Raper SCB, Watterson IG, Weaver AJ, Zhao Z-C (2007) Global climate projections. In: Solomon S, Qin D, Manning M, Chen Z, Marquis M, Averyt KB, Tignor M, Miller HL (eds) Climate change 2007: the physical science basis. Contribution of working group I to the fourth assessment report of the Intergovernmental Panel on Climate Change. Cambridge University Press, Cambridge

Raphael MN (2003) The Santa Ana winds of California. Earth Interact 7:1–13

Schär C, Vidale PL, Lüthi D, Frei C, Häberli C, Liniger MA, Appenzeller C (2004) The role of increasing temperature variability in European summer heatwaves. Nature 427:332–336

Saunders IR, Byrne JM (1999) Using surface and geopotential height fields for generating grid-scale precipitation. Int J Climatol 19:1165–1176

Schoof JT, Pryor SC (2003) Evaluation of the NCEP-NCAR reanalysis in terms of synoptic-scale phenomena: a case study from the Midwestern USA. Int J Climatol 23:1725–1741

Sheppard PR, Comrie AC, Packin GD, Angersbach K, Hughes MK (2002) The climate of the US Southwest. Clim Res 21:219–238

Sheridan SC (2002) The redevelopment of a weather type classification scheme for North America. Int J Climatol 22:51–68

Sheridan SC, Kalkstein AJ (2010) Seasonal variability in heat-related mortality across the United States. Nat Hazard 55:291–305

Sheridan SC, Kalkstein LS (2004) Progress in heat watch-warning system technology. Bull Am Meteorol Soc 85:1931–1941

Sheridan SC, Kalkstein AJ, Kalkstein LS (2009) Trends in heat-related mortality in the United States, 1975–2004. Nat Hazard 50:145–160. doi:10.1007/s11069-008-9327-2

Sheridan SC, Lee CC (2010) Synoptic climatology and the general circulation model. Prog Phys Geogr 34:101–109

Stone DA, Weaver AJ, Stouffer RJ (2001) Projection of climate change onto modes of atmospheric variability. J Clim 14:3551–3565

Stott PA, Stone DA, Allen MR (2004) Human contribution to the European heatwave of 2003. Nature 432:610–613

Tebaldi C, Hayhoe K, Arblaster JM, Meehl GA (2006) Going to extremes, an intercomparison of model-simulated historical and future changes in extreme events. Clim Chang 79:185–211

Vrac M, Hayhoe K, Stein M (2007) Identification and intermodal comparison of seasonal circulation patterns over North America. Int J Climatol 27:603–620

Wetterhall F, Bárdossy A, Chen D, Halldin S, Xu C (2009) Statistical downscaling of daily precipitation over Sweden using GCM output. Theor Appl Climatol 96:95–103

Willett KM, Sherwood S (2011) Exceedance of heat index thresholds for 15 regions under a warming climate using the wet-bulb globe temperature. Int J Climatol in press doi:10.1002/joc.2257